Technologies and Materials for Renewable Energy, Environment & Sustainability

# Synthesis, and Structural Investigations of TiO2 Doped Cr2O3 Thin Films for Gas Sensor Applications

AIPCP25-CF-TMREES2025-00007 | Article

PDF auto-generated using **ReView** from

RIVER VALLEY TECHNOLOGIES

# Synthesis, and Structural Investigations of $TiO_2$ Doped $Cr_2O_3$ Thin Films for Gas Sensor Applications

Nihad K. Ali[1, a)] and Ikhlas H. Shallal[1, b)]

[1] *Department of Physics, College of Education for Pure Science /Ibn Al-Haitham, Baghdad University, Baghdad, Iraq*

[a)] *Corresponding author: nihad.ali2304@ihcoedu.uobaghdad.edu.iq*
[b)] *akhlas.h.s@ihcoedu.uobaghdad.edu.iq*

**Abstract.** The most important details of the synthesis by using pulsed laser ablation in deionized water to ablate the $Cr_2O_3$ and $TiO_2$ nanoparticles and drop-casting the solutions on the substrates to deposit $Cr_2O_3$ thin films with concentration ratio (0, 0.2, 0.4, 0.6, 0.8) % of $TiO_2$ are illustrated. Additionally, a concise and precis explanation of the structural analysis included X-ray diffraction (XRD) and atomic force microscopy (AFM) and gas sensor performance evaluation were provided. (XRD) test revealed that all samples of $Cr_2O_3$:$TiO_2$ films have a polycrystalline nature with Rhombohedral structure and the $Cr_2O_3$ is crystalized as a main plane in (012), while $TiO_2$ nanoparticles have anatase phase with tetragonal crystal structure at plane (112). The gas sensor device of the heterojunction of $Cr_2O_3$:$TiO_2$/Psi with concentration ratio (0, 0.2, 0.4, 0.6, 0.8) % of $TiO_2$ were examined when exposed to 400ppm of $NO_2$ gas at various temperatures (R.T, 100, 150) °C. The maximum value of sensitivity was 475.11% detected at 0.6% $TiO_2$ at operation temperature of 100°C.
**Keywords:** thin films, Structural, gas sensing, $Cr_2O_3$:$TiO_2$, laser ablation.

## INTRODUCTION

In recent years, discussions regarding metal oxide semiconductors (MOs) have dominated research, due to them distinct optical, magnetic, and electrical characteristics [1]. As with all oxides of metal, chromium (III) oxide has critically influenced academic dialogue either a nano-powder or thin film [2]. Chrome oxides like $CrO_2$ and $Cr_2O_3$ and chromium (Cr)–titanium (Ti) interaction types, have several states according to the applied power on the chromium metallic phase and shows peaks with high energy due to its significant intrinsic characteristics. In the last two decades the most transition oxide that had been studied is titanium oxide which is required in many areas of applications like solar cells, gas sensors and transparent electrodes [3]. Because of $Cr_2O_3$ diverse properties, it falls under the most stable phases and the hardest transition MOs which enabled it to be a unique industrial material [4]. Where it has a high melting point (2473K), resistance the oxidation at elevated temperatures, and large optical absorbance [5]. Chromium trioxide ($Cr_2O_3$), is a p-type semiconductor with a wide optical energy gap, excess oxygen, and a refractive index with a high value [6]. In this regard, titanium dioxide ($TiO_2$) also known as an MOs with high refractive index, photocatalytic efficiency, and chemical stability [7], both $Cr_2O_3$ and $TiO_2$ are employed as thin films and sensing species in gas sensors according to their properties and advantages of low cost, tiny size and operation at ease and good ability to reverse and long life, good and reliability for real-time applications when compared with other gas sensing devices. [8]. The substantial mechanism of gas sensors based on metal oxide semiconductor thin films depends on electrical resistance that changes during the interaction between the sensor's material surface and the molecules of the absorbed gas, overall, two functions occur in chemical sensors, firstly receptor function to detect and distinguish the gas, secondly transducer function to obtain output signal from the chemical signal [9]. Various techniques were utilized for producing gas sensor thin films. As Thermal evaporation [10], sol-gel [11], spin-coating [12], pulsed laser deposition (PLD) [13,14] R.F magnetron sputtering [15], spray pyrolysis [16,17] and hydrothermal method [18].

This work aims to investigate the effect of adding $TiO_2$ dopant to $Cr_2O_3$ nanoparticles deposited by implemented pulsed laser ablation in liquid (PLAL) and drop-casting techniques to explore the structural and gas sensing properties.

## EXPERIMENTAL TECHNIQUES

To ablate the nanoparticles ($NP_S$) of the chromium trioxide ($Cr_2O_3$) and titanium dioxide ($TiO_2$) via pulse laser ablation in liquid (PLAL). First, High purity powders with purity (99.999%) which were supplied by (Central Drug House, India) company and (Sigma –Aldrich, China) company respectively were weighed as 7g of $Cr_2O_3$ and 2g of $TiO_2$. Then, they were compacted by the hydraulic compressor under a pressure of 12 Ton with a duration of 24 hours to create pellets with a diameter of 1.7cm. The pellet was placed at the bottom of a glass beaker that contains 20ml of deionized water and it was irradiated by Nd:YAG pulsed laser type (Huafei) with 1064nm wavelength and laser energy of 600mJ for 500 pulses , pulses frequency 8Hz . A converging lens of 10cm focal length was used to focus the laser beam as a spot with a diameter of 2.3mm on the target surface, After the continuing of the ablation process and rotating the beaker, a colloidal solution was prepared, To synthesis the doped thin films, the colloidal solutions with volume of $Cr_2O_3$ (9.98 , 9.96 , 9.94 , 9.92)ml and $TiO_2$ with (0.02 , 0.04, 0.06 , 0.08)ml were sequentially mixed, The drop casting method was used to deposit films by dropping 1ml of each colloidal solution on a glass and n-type porous silicon substrates with dimensions of $(1.5\times1.5)cm^2$ at a temperature of 400℃, the liquid evaporates by the heating effect to form the thin film with thickness 200nm. Structural and sensitivity measurements were recorded for $Cr_2O_3$ films doped with (0.2, 0.4, 0.6, 0.8) % of $TiO_2$ ratios. X-ray diffraction analysis technique model PHILIPS PW 1730, The Netherland, Cu-Kα radiation (λ=1.54060nm) operated on a tube voltage of 40KV and current of 30A was employed to characterize the crystalline structure for the prepared films, the scan angle was changed within the range from 10deg to 80deg with a step size of 0.05deg, The morphology of thin films surface was studied by atomic force microscopy (TT-2 AFM Workshop, USA.). Gas-sensing measurements which included, the resistance of thin films in the presence of $NO_2$ gas with a concentration of 400ppm, The $NO_2$ gas sensitivity, response, and recovery times of the samples were calculated and discussed. Figure 1. illustrates a simple diagram of the experimental (PLAL system).

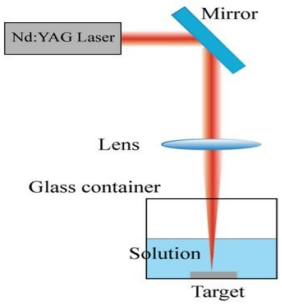


**FIGURE 1.** Pulsed laser ablation in liquid system.

## RESULTS AND DISCUSSION

### Structural characterization

The structural characterization of the prepared thin films was studied using the results of x-ray diffraction (XRD) and atomic force microscopy (AFM) analyses.

### X-ray diffraction spectrum

The x-ray diffraction spectrum was employed to characterize the crystallographic features of the as-deposited

thin films. Debye Scherrer's equation was utilized to compute the crystallite sizes in nm [19]:

$$Crystalline\ size\ (C.s) = \frac{(0.94)\lambda}{\beta \cos\theta} \quad (1)$$

where (0.94) is the Scherer's constant, λ is the X-ray wavelength in nm, and the full width at half maximum (FWHM) is symbolized as β in radian.The pure and doped $Cr_2O_3$ thin films yielded a polycrystalline nature and the $Cr_2O_3$ is crystalized as Rhombohedral structure according to ICDD card NO. 00-006-0504, with a main phase in plane (012) corresponding to 2θ = 24.543° and the plane (202) in the concentration (0.4% and 0.6%) which belongs to $TiO_2$ corresponding to 2θ = 44.143° ,and 44.193° respectively. The secondary phase $CrO_3$ with orthorhombic structure was surfaced at the concentration (0% , 0.2% , 0.4% , 0.6%) of $TiO_2$ in the plan (200) based on ICDD card NO. 00-032-6285 , May be the appearance of the secondary phase was the deposition conditions where the redox behavior was foreseen [20] , A new peak was observed in (0.8%) $TiO_2$ thin film at plane (112) and 2θ = 38.593° indicates the dopant $TiO_2$ Anatase phase with tetragonal crystal system compared with ICDD card NO. 21-1272 ,The nanoparticles of $Cr_2O_3$ crystalline size where decreased along (012)plane ,with increasing $TiO_2$ concentration from 33.66 nm for 0.2% $TiO_2$ to 21.69nm for 0.8% $TiO_2$ and the same behavior at plane (202) was decreased from 21.04 nm for the sample of 0.4% $TiO_2$ to 20.79nm for 0.6% $TiO_2$, the increasing of $TiO_2$ dopant concentration ratio influenced by decreasing peaks intensity this might be due to the existence $Ti^{4+}$ ions in $Cr_2O_3$ lattice and substitute $Cr^{3+}$ ions [21]. Figure 2. illustrates XRD patterns of pure and doped $Cr_2O_3$ thin films.

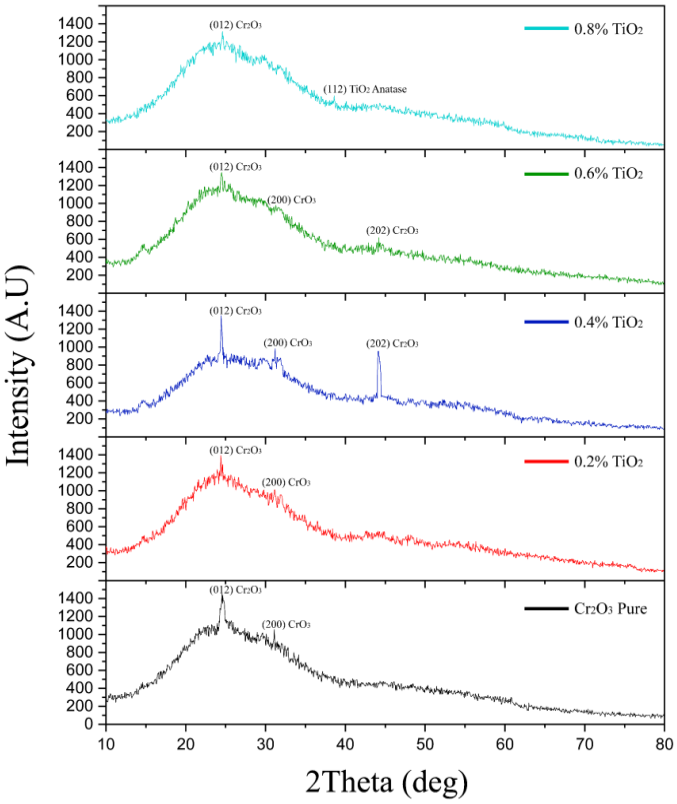


**FIGURE 2.** XRD pattern of pure and doped $Cr_2O_3$ thin films.

## ATOMIC FORCE MICROSCOPY (AFM)

The morphology of deposited thin films and surface roughness was detected by AFM 3D images fig. 3. which clearly shows granular topography, where granular nanostructures have high surface area which provides more interaction sites with gas molecules and as a result the gas sensitivity increases with a proportional relationship [22], the pure $Cr_2O_3$ thin film exhibited the lowest grain size (30.16nm) which shows an inconsistent increase in the doped $Cr_2O_3$ thin film relative to the pure $Cr_2O_3$ thin film with increasing the ratio of $TiO_2$ dopant (0.2 % , 0.4 % , 0.6% , 0.8 %) , the grain size increased to 77.10nm after doping with ratio of 0.2 % $TiO_2$ followed by decrease in values of 48.79nm and 42.78nm in ratio of 0.4% and 0.6% $TiO_2$ respectively , the reason might be the scattering of grain boundaries resulting from crystalline degradation of thin films [23] , and increase to 85.02nm at ratio 0.8% $TiO_2$. The doped sample with ratio 0.2% showed the highest value of mean roughness of 19.65nm and root mean square (RMS) of 27.12nm and the 0.8% $TiO_2$ doped thin film recorded mean roughness of 10.92nm and RMS of 15.03nm. Table 1. represents the AFM parameters for pure and doped $Cr_2O_3$ thin films. The reason of the increase in roughness might be due to the random distribution of the faceted hillocks on the relatively smooth structure and densification of the deposition procedures [24].

**TABLE 1.** AFM parameters for pure and doped $Cr_2O_3$ thin films.

| Sample | RMS (nm) | Mean Roughness (nm) | Average Grain Size (nm) |
|---|---|---|---|
| $Cr_2O_3$/PSi | 10.20 | 8.61 | 30.16 |
| $Cr_2O_3$: (0.2%)$TiO_2$/PSi | 27.12 | 19.65 | 77.10 |
| $Cr_2O_3$: (0.4%)$TiO_2$/Psi | 10.00 | 7.86 | 48.79 |
| $Cr_2O_3$: (0.6%) $TiO_2$/Psi | 10.14 | 7.99 | 42.78 |
| $Cr_2O_3$: (0.8%)$TiO_2$/PSi | 15.03 | 10.92 | 85.02 |

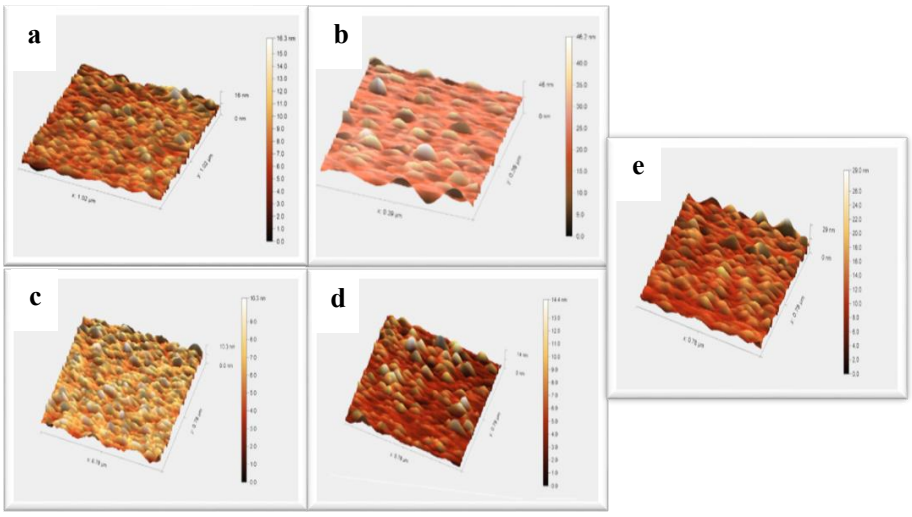


**FIGURE 3.** AFM images for pure and doped $Cr_2O_3$ thin films.
a) 0% $TiO_2$ b) 0.2% $TiO_2$ c) 0.4% $TiO_2$ d) 0.6% $TiO_2$ e) 0.8% $TiO_2$

## GAS SENSOR PROPERTIES

The gas sensor device prepared from the heterojunction of $Cr_2O_3$:$TiO_2$/Psi with concentration ratio (0 , 0.2 , 0.4 , 0.6 , 0.8)% of $TiO_2$ were examined when exposed to 400ppm of $NO_2$ gas at various temperatures (R.T , 100 , 150)°C , the resistance for as-sensors where decrease when exposed to $NO_2$ oxidizing gas as a typical behavior of P-type semiconductor nature due to the increasing of the positive holes concentration as a result for introduction the negative charge of adsorbed oxygen ions and the molecules of the targeted gas [ 25,26 ] , as shown in figs. 4 and 5.

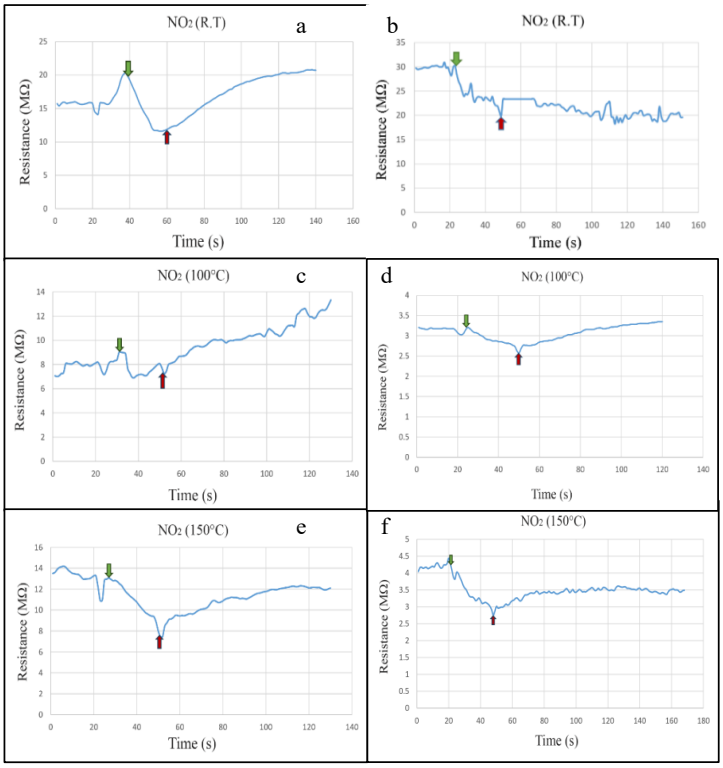


**FIGURE 4a,b,c,d,e,f.** Resistance variation with time of thin films in three different operation temperatures for:
I - Pure $Cr_2O_3$ II - $Cr_2O_3$:(0.2%) $TiO_2$

Table (2) shows the sensitivity behavior that increases from 51.60 % to 158.80% when concentration ratio of TiO2 was increased from 0% to 0.4% in a different operation temperature. it might be the doping effect of metal oxide layer with other metal oxide which enhances the sensing characteristics [27].
The maximum value of sensitivity was 475.11% detected at 0.6% $TiO_2$ at operation temperature of 100°C, it could be the synergistic effect of heterojunction where the gas molecules react with adsorbed oxygen ions in first material of the junction and the by-product may readily react with the oxygen ions in the second material to complete the reaction [28]. Figure 6. clarify the variation of sensitivity for $NO_2$ as a function to the $TiO_2$ dopant ratio.
Doping with elements can affect the surface defects and electrical properties of the sensor material, enhancing electron transfer. At the same time, doping with elements can alter the band gap of the material, thereby improving its gas sensitivity. In particular, doping with metals with high catalytic activity and low Fermi levels will stimulate electronic and chemical sensing, effectively improving the material's gas sensitivity [29]. formed titanium dioxide nanofiber films doped with palladium with varying amounts of doping using a flame surface stabilization (FSRS) technique. It

was found that doping with noble metals enhanced the response intensity of the titanium dioxide-based sensor to carbon monoxide gas, while also significantly reducing its response/recovery times to ammonia gas [30].

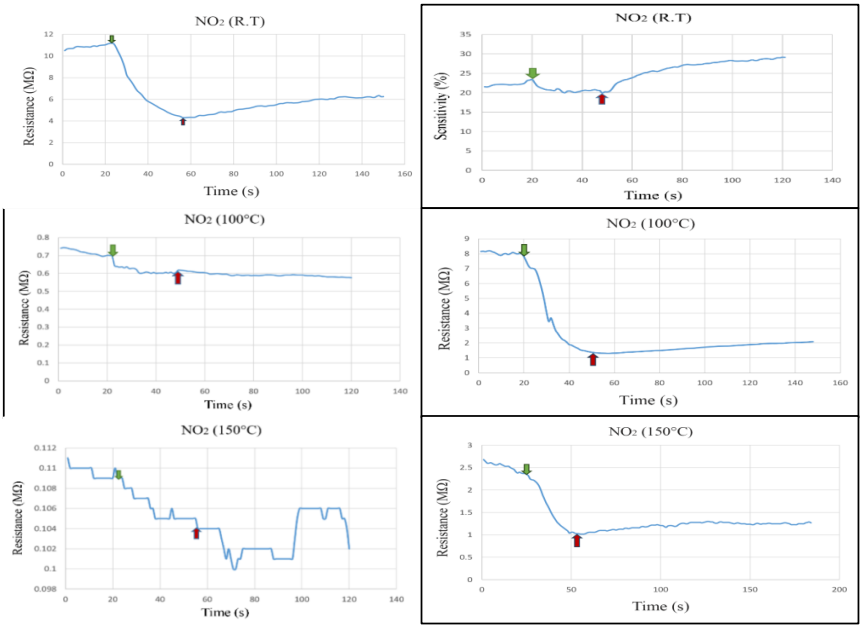


(a) (b)

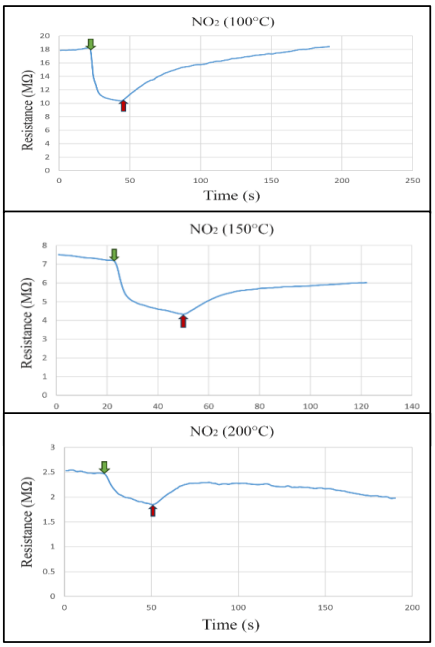


(c)

**FIGURE 5.** resistance variation with time of thin films in three different operation temperature for:
a- $Cr_2O_3$:(0.4%) $TiO_2$ b - $Cr_2O_3$:(0.6%) $TiO_2$ c - $Cr_2O_3$:(0.8%) $TiO_2$

**TABLE 2.** Sensitivity characteristics of $Cr_2O_3$:$TiO_2$/PSi at different operation temperature.

| Sample | Operating Temp.(℃) | Sensitivity (%) | Response Time (s) | Recovery Time (s) |
|---|---|---|---|---|
| $Cr_2O_3$/PSi | R.T | 51.60 | 23.4 | 90.9 |
| | 100 | 23.26 | 21.6 | 63 |
| | 150 | 50.00 | 25.2 | 45.9 |
| $Cr_2O_3$: (0.2%)$TiO_2$/PSi | R.T | 67.00 | 18.9 | 81 |
| | 100 | 24.24 | 18.9 | 61.2 |
| | 150 | 72.99 | 23.4 | 61.2 |
| $Cr_2O_3$: (0.4%)$TiO_2$/PSi | R.T | 158.80 | 29.7 | 84.6 |
| | 100 | 12.78 | 25.2 | 45 |
| | 150 | 4.81 | 30.6 | 39.6 |
| $Cr_2O_3$: (0.6%) $TiO_2$/PSi | R.T | 17.46 | 25.2 | 64.8 |
| | 100 | 475.11 | 27.9 | 62.1 |
| | 150 | 125.96 | 24.3 | 61.2 |
| $Cr_2O_3$: (0.8%)$TiO_2$/PSi | 100 | 75.34 | 19.8 | 68.4 |
| | 150 | 66.51 | 25.2 | 45 |
| | 200 | 33.87 | 27 | 44.1 |

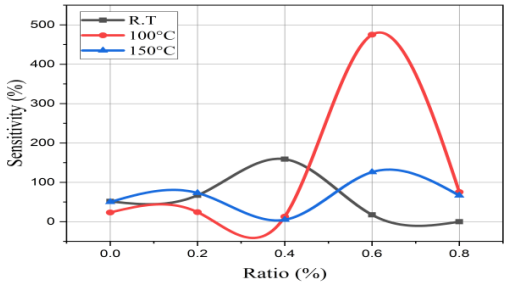


**FIGURE 6.** shows the variation of sensitivity for $NO_2$ as a function of dopant ratio.

The sample doped by 0.8% $TiO_2$ didn't show a sensitivity for $NO_2$ gas at room temperature but detected a good value of sensitivity (75.34%) at 100°C , the response time and recovery time changed in different values relative to $TiO_2$ concentration in thin films but recorded the lowest response time magnitude (18.9s) at 0.2% $TiO_2$ concentration thin film at both room temperature and 100°C, while the minimum recovery time was 39.6s for the sample with concentration of 0.4% $TiO_2$ at 150°C.

## CONCLUSIONS

$Cr_2O_3$ thin films pure and doped by $TiO_2$ with contained ratio (0 , 0.2 , 0.4 , 0.6 , 0.8)% were synthesized by using pulsed laser ablation in liquid and drop-casting processes step by step. X-ray diffraction (XRD), revealed that all samples of $Cr_2O_3$:$TiO_2$ films have a polycrystalline nature with Rhombohedral structure with main plane in (012),while $TiO_2$ nanoparticles have Anatase phase with tetragonal crystal structure. The maximum sensitivity value of gas sensor device of $Cr_2O_3$: 0.6% $TiO_2$/Psi for $NO_2$ gas was 475.11% detected at operation temperature of 100°C. The high performance of as fabricated gas sensor indicated that it is promising for $NO_2$ sensitivity toward air quality

which make it a good candidate for investment in environmental monitoring and industrial gasses hazards trucker also it can be utilized in cross-sensitivity tests.

## ACKNOWLEDGEMENTS

The authors extend their sincere gratitude to the Department of Physics at the College of Education for Pure Science/Ibn Al-Haithem, University of Baghdad for their support. We also deeply appreciate to dr. morooj A. Aboode\Solar Energy Research Center, Renewable Energy Directorate\Iraq, for her assistance.

## REFERENCES

1. M. H. Suhail, I. K. Adehmash, S. M. Abdul Kareem, D. A. Tahir, and O. G. Abdullah, *Trans. Electr. Electron. Mater.* **21**, 327 (2020).
2. A. Zekaik, H. Benhebal, and B. Benrabah, *High Temp. Mater. Proc.* **38**, 806 (2019).
3. A. Hajjaji, M. Amlouk, M. Gaidi, B. Bessais, and M. A. El Khakani, Chromium Doped $TiO_2$ Sputtered Thin Films: Synthesis, Physical Investigations and Applications (Springer, Cham, 2015).
4. A. Kadari, T. Schemme, D. Kadri, and J. Wollschläger, *Results Phys.* **7**, 3124 (2017).
5. A. K. Panda, A. Singh, R. Divakar, N. G. Krishna, V. R. Reddy, and R. Thirumurugesan, *Thin Solid Films* **660**, 328 (2018).
6. J. Singh, V. Verma, R. Kumar, and R. Kumar, *Mater. Res. Express* **6**, 096414 (2019).
7. H. Chen, B. A. Prastika, Z. Zhang, and C. Zhang, *Appl. Phys. A* **131**, 134 (2025).
8. J. Cao, Y. Xu, L. Sui, X. Zhang, S. Gao, and X. Cheng, *Sens. Actuators B Chem.* **220**, 1146 (2015).
9. S. Ponmudi, R. Sivakumar, C. Sanjeeviraja, C. Gopalakrishnan, and K. Jeyadheepan, *Appl. Surf. Sci.* **463**, 556 (2019).
10. S. H. Salman, N. A. Hassan, and G. S. Ahmed, *Chalcogenide Lett.* **19**, 125 (2022).
11. S. A. Kadhim and T. M. Al-Saadi, *Ibn Al-Haitham J. Pure Appl. Sci.* **36**, 159 (2023).
12. I. A. Kareem and H. F. Oleiwi, *Ibn Al-Haitham J. Pure Appl. Sci.* **36**, 137 (2023).
13. M. A. Abood and B. A. Hasan, *Iraqi J. Sci.* **64**, 1675 (2023).
14. A. J. Haider, R. H. Al-Anbari, G. R. Kadhim, and C. T. Salame, "Exploring potential environmental applications of $TiO_2$ nanoparticles," Energy Procedia 119, 332–345 (2017).
15. S. H. Salman, A. A. Shihab, and A. K. Elttayef, *Energy Procedia* **157**, 283 (2019).
16. Q. G. Al-zaidi, A. M. Suhail, and W. R. Al-azawi, *Appl. Phys. Res.* **3**, 89 (2011).
17. A. H. A. Alrazak, S. H. Salman, I. A. Abbas, M. H. Mustafa, H. M. Ali, and S. A. Abbas, *Dig. J. Nanomater. Biostruct.* **20**, 191 (2025).
18. S. A. Hamdan and I. M. Ali, *Baghdad Sci. J.* **16**, 0221 (2019).
19. S. S. Mahmood, B. A. Hasan, and A. F. Rauuf, *Iraqi J. Sci.* **65**, 3754 (2024).
20. V. B. Kamble and A. M. Umarji, *J. Mater. Chem. C* **1**, 8167 (2013).
21. T. C. Kaspar, P. V. Sushko, M. E. Bowden, S. M. Heald, A. Papadogianni, and C. Tschammer, *Phys. Rev. B* **94**, 155409 (2016).
22. N. G. Deshpande, Y. G. Gudage, R. Sharma, J. C. Vyas, J. B. Kim, and Y. P. Lee, "Studies on tin oxide-intercalated polyaniline nanocomposite for ammonia gas sensing applications," *Sensors and Actuators B: Chemical* **138**, 76 (2009).
23. N. Manjula, M. Pugalenthi, V. S. Nagarethinam, K. Usharani, and A. R. Balu, *Mater. Sci.-Pol.* **33**, 774 (2015).
24. S. M. Abdulkareem, M. H. Suhail, and I. K. Adehmash, *Iraqi J. Sci.* **62**, 2176 (2021).
25. F. El Haj Hassan, S. Moussawi, W. Noun, C. Salame, and A. V. Postnikov, "Theoretical calculations of the high-pressure phases of $SnO_2$," Comput. Mater. Sci. 72, 86–92 (2013).
26. Aleabi, S.H., Watan, A.W., Salman, E.M.-T., kareem Jasim A.,Shaban, A.H., Alsaadi, T.M., AIP Conference Proceedings, 2018, 1968, 020019.
27. N. Dasgupta, S. Ranjan, and E. Lichtfouse, eds., *Environmental Nanotechnology Volume 3* (Springer, 2020).
28. M. K. Jayaraj, ed., Nanostructured Metal Oxides and Devices: Optical and Electrical Properties (Springer, Singapore, 2020).
29. Ahmed BA, Mohammed JS, Fadhil RN, Shaban AH, Al Dulaimi AH. *Chalcogenide Lett*. 2022;19(4):301-308.
30. Salman SH, Jahil SS, Hassan NA, Abbas SA, Jasim KA. Ammonia gas sensing using porous silicon. *J Phys Conf Ser*. 2024;2857(1):012051